JACS
JOURNAL OF THE AMERICAN CHEMICAL SOCIETY
Article
pubs.acs.org/JACS

An Operationally Simple and Mild Oxidative Homocoupling of Aryl Boronic Esters To Access Conformationally Constrained Macrocycles

Evan R. Darzi,[†] Brittany M. White,[†] Lance K. Loventhal,[†] Lev N. Zakharov,[‡] and Ramesh Jasti*[,†]

[†]Department of Chemistry and Biochemistry & Materials Science Institute, University of Oregon, Eugene, Oregon 97403, United States

[‡]CAMCOR, University of Oregon, Eugene, Oregon 97403, United States

Supporting Information

ABSTRACT: Constrained macrocyclic scaffolds are recognized as challenging synthetic motifs with few general macrocyclization methods capable of accessing these types of systems. Although palladium catalyzed oxidative homocoupling of aryl boronic acids and esters to biphenyls has been recognized as a common byproduct in Suzuki–Miyaura cross-couplings for decades, this reactivity has not been leveraged for the synthesis of challenging molecules. Here we report an oxidative boronic ester homocoupling reaction as a mild method for the synthesis of strained and conformationally restricted macrocycles. Higher yields and better efficiencies are observed for intramolecular diboronic ester homocouplings when directly compared to the analogous intramolecular Suzuki–Miyaura cross-couplings or reductive Yamamoto homocouplings. Substrates included strained polyphenylene macrocycles, strained cycloalkynes, and a key macrocyclic intermediate toward the synthesis of acerogenin A. Notably, this oxidative homocoupling reaction is performed at room temperature, open to atmosphere, and without the need to rigorously exclude water, thus representing an operationally simple alternative to traditional cross-coupling macrocyclizations. The mechanism of the reaction was investigated indicating that 1–5 nm palladium nanoparticles may serve as the active catalyst.

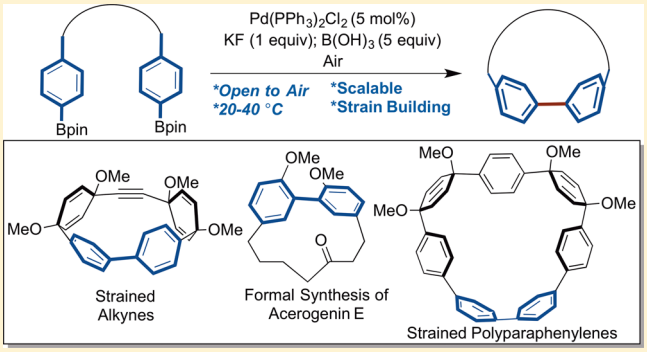

INTRODUCTION

Macrocyclic molecules are widely recognized as useful structural motifs across disciplines including materials science,[1] medicinal chemistry,[2] and supramolecular chemistry.[3] Synthetic methods toward efficient macrocycle formation, however, remain a challenge and often represent the limiting step in a synthetic sequence. This limitation becomes increasingly apparent when the desired macrocycle is sterically congested, conformationally restricted, or distorted from ideal geometry. Examples of challenging biaryl-containing macrocycles range from natural products such as haouamine A[4] or vancomycin[5] to the "bent and battered" benzene rings found in cyclophanes.[6] Moreover, the strain and conformational restriction imparted by the macrocyclic motif is often directly responsible for the desirable properties. Examples include the strain-induced narrowing of the HOMO–LUMO gap in [*n*]cycloparaphenylenes ([*n*]CPPs),[7] strain releasing ring-opening metathesis polymerization of various monomers,[1a,c] and restricted conformational flexibility of macrocycles that can increase drug binding for medicinal chemistry applications.[2b] For these reasons, constrained macrocycles have served as motivation for developing methodolgy to construct these challenging systems under mild transition metal catalyzed conditions.

Typical transition metal catalysis for intramolecular biaryl coupling can be divided into three classes as shown in Figure 1a.[8] First, a redox neutral cross-coupling of a nucleophile and electrophile can generate strained biaryl macrocycles as in the case of a Suzuki–Miyaura, Negishi, and Stille cross-coupling. A second possibility is a reductive coupling which can be used to bring two electrophilic ends together to provide the desired macrocyclic structure as in the case of the Yamamoto coupling. Finally, there is the oxidative homocoupling of nucleophiles such as the widely used Glaser–Hay reaction used to form diynes. The downsides for the first two approaches are the need for an inert oxygen-free environment and typically more forcing conditions in order to accommodate the oxidative insertion step. The downsides of the latter nucleophilic couplings are the need for toxic reagents (organostannane or organomercury) or highly reactive organometallics (lithiates, grignards, or cuprates) which are incompatible with protic solvents or substrates with acidic protons.

In 2014, we observed strained macrocycle **2** as a byproduct in an attempted Suzuki–Miyaura cross-coupling utilizing diboronic ester **1** (Figure 1b).[9] This palladium catalyzed reaction was found to operate efficiently at room temperature and open to air. The oxidative homocoupling was the key development leading to the synthesis and characterization of [5]CPP, a

Received: December 8, 2016
Published: February 2, 2017

DOI: 10.1021/jacs.6b12658
J. Am. Chem. Soc. 2017, 139, 3106–3114

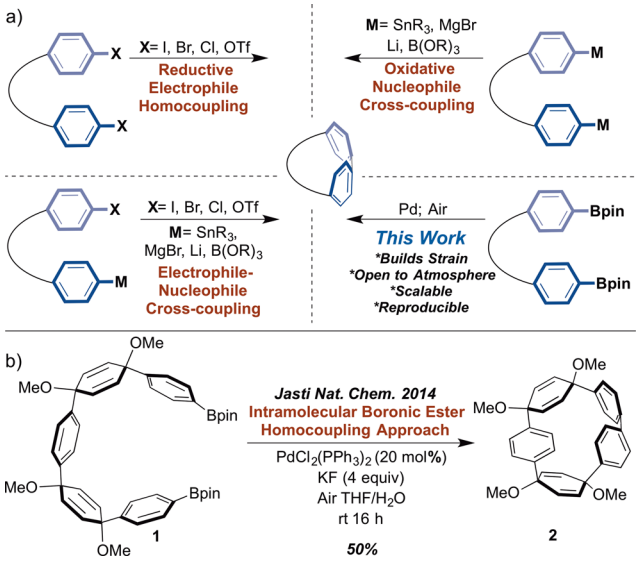

Figure 1. (a) Common intramolecular macrocyclization strategies and (b) the recently disclosed oxidative homocoupling reaction to form a highly strained macrocycle.

highly strained molecular fragment of C_{60} (118 kcal/mol of strain energy). Although this oxidative homocoupling process has long been appreciated as a side product in Suzuki–Miyaura cross-coupling reactions, minimal efforts have been devoted into exploring this reaction in the context of complex molecule synthesis.[10] The major exception to this is the pioneering work by Merlic and co-workers on the oxidative homocoupling of vinyl boronic esters in the synthesis of complex cyclic dienes.[11] Herein we provide a detailed study of this oxidative aryl–aryl bond forming reaction in order to optimize reaction conditions, explore the generality and scope of substrates, and probe the reaction mechanism. This study establishes this reaction as an operationally simple alternative to traditional cross-coupling reactions, with the capability of constructing challenging macrocycles ranging from cyclophanes to strained alkynes to conformationally restricted natural products. Our mechanistic work also suggests the strong possibility of 1–5 nm palladium particles serving as the catalytic species.

RESULTS AND DISCUSSION

At the outset of these studies, we first considered the mechanistic history of this oxidative homocoupling process. The first mechanistic study was performed in 1994 by Pleixitas implicating an initial oxidative insertion into $Ar–B(OH)_2$ followed by a transmetalation of a second equivalent of $ArB(OH)_2$ and finally reductive elimination to give the homocoupled product.[12] In 2005 Adamo et al. proposed an alternative mechanism utilizing DFT calculations to support experimental observations (Figure 2).[13] The catalytic cycle begins with the oxidation of a bis-ligated palladium(0) to form palladium(II) di(triphenylphosphine)peroxide **3** (step **A**). This peroxo intermediate was first suggested by Yoshida[14] and had previously been synthesized on a large scale by simple oxygenation of $Pd(PPh_3)_4$.[15] After palladium peroxo activation, one of the palladium bound oxygens can coordinate an aryl boronic acid or ester (step **B**). This facilitates the first transmetalation of an aryl group to give a boronic peroxo species (step **C**). Importantly, this first transmetallaton step was found both theoretically and experimentally to be second order

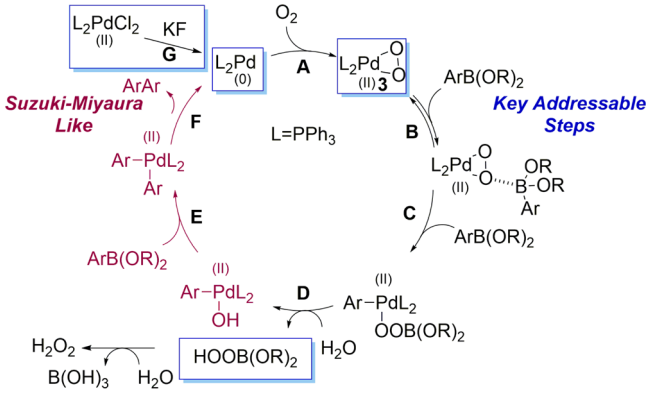

Figure 2. Proposed catalytic cycle by Adamo et al.[13]

in boronic acid.[13a] Water or an alternative nucleophile can then attack this peroxide intermediate to give a palladium hydroxo species and 1 equiv of hydrogen peroxide (step **D**). This palladium hydroxo species is closely related to the pretransmetalation intermediate for Suzuki–Miyaura cross-coupling.[16] In fact, the mechanism is nearly identical to the classical Suzuki–Miyaura mechanism from this palladium hydroxo species through the terminal reductive elimination (steps **E** and **F**).[17] Although the existence of the palladium hydroxo intermediate in Suzuki–Miyaura has been debated, Denmark recently showed strong experimental support for such a pretransmetalation intermediate.[18] The key addressable points in the catalytic cycle in Figure 2 are highlighted in blue and are discussed in more detail in the following paragraphs.

Reaction Optimization. With the initial observation of an efficient room temperature oxidative homocoupling of **1** to give macrocyclic structure **2** in hand and a greater appreciation for the proposed catalytic cycle, we began to probe various parameters to optimize this reaction. These results are summarized in Table 1. We initially explored other group 10 transition metals, nickel (entry 2) and platinum (entry 3), with the same conditions and ligand system reported for palladium (entry 1). Neither bis(triphenylphosphine)nickel(II) dichloride nor bis(triphenylphosphine)platinum dichloride provided any conversion to product. Two primary reasons for the lack of observed reactivity with nickel and platinum can be proposed. First, Verkade[19] showed that fluoride could be used to efficiently reduce $PdCl_2(PPh_3)_2$ to the corresponding $Pd(PPh_3)_4$ (step **G**) in the presence of excess triphenylphosphine; however, no such reactivity was observed for Ni(II) and only sluggish reduction of Pt(II) was observed. Second, Roth[20] demonstrated the rate of oxygenation of a variety of $M(PPh_3)_4$ complexes in solution including Ni, Pd, and Pt. Interestingly, palladium binds O_2 with a rate constant over an order of magnitude higher than Ni or Pt, also consistent with Pd being the superior group 10 transition metal for this transformation.

Next a variety of palladium(II) ligand systems were screened (entries 4–7). These ligands were chosen to encompass a wide range of ligand structures including N-heterocyclic carbenes (NHCs), bidentate phosphines, and bulky phosphine ligands. Interestingly, there was little variance in conversion and yield when alternate phosphine ligands were used; however, NHCs and other nitrogen based ligands were ineffective. This supports the fluoride-mediated reduction of the various palladium species through the oxidation of the phosphine ligands to their corresponding phosphine oxides.[19] The insensitivity to

DOI: 10.1021/jacs.6b12658
J. Am. Chem. Soc. 2017, 139, 3106–3114

Table 1. Optimization of Oxidative Homocoupling of Diboronic Ester 1 to Strained Macrocycle 2

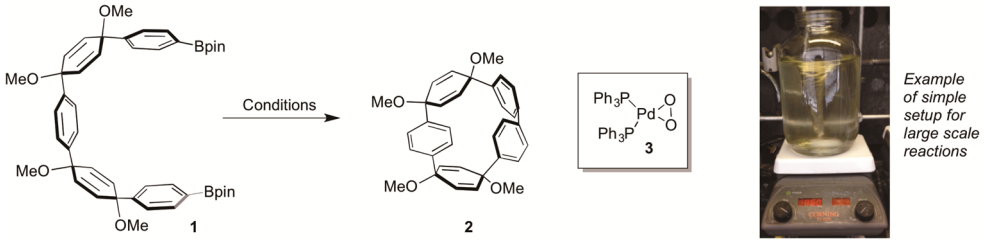

entry	catalyst	base	oxidant	conversion[a]	yield[b]
1	$PdCl_2(PPh_3)_2$ (20 mol %)	KF (4 equiv)	air	100	50
2	$NiCl_2(PPh_3)_2$ (20 mol %)	KF (4 equiv)	air	10	0
3	$PtCl_2(PPh_3)_2$ (20 mol %)	KF (4 equiv)	air	20	0
4	Pd(dppf)Cl_2 (20 mol %)	KF (4 equiv)	air	100	40
5	Pd(dppp)Cl_2 (20 mol %)	KF (4 equiv)	air	100	30
6	Pd(PEPPSI)(SiP) (20 mol %)	KF (4 equiv)	air	60	25
7	$Pd(OAc)_2$ (20 mol %)	KF (4 equiv)	air	40	20
8	$PdCl_2(PPh_3)_2$ (20 mol %)	KF (4 equiv)	benzoquinone	100	0
9	$PdCl_2(PPh_3)_2$ (20 mol %)	KF (4 equiv)	Cu(II)Cl	90	0
10	$PdCl_2(PPh_3)_2$ (20 mol %)	KF (4 equiv)	O_2 (g)	100	45
11	$Pd(PPh_3)_4$ (20 mol %)	N/A	air	100	40
12	$Pd(OAc)_2$ (20 mol %)	SPhos (50 mol %)	air	100	50
13	$Pd(dba)_2$ (20 mol %)	N/A	air	100	40
14	(η-O_2)$Pd(PPh_3)_2$ (20 mol %)	N/A	air	80	42
15	(η-O_2)$Pd(PPh_3)_2$ (5 mol %)	N/A	air	25	25
16	(η-O_2)$Pd(PPh_3)_2$ (20 mol %)	$NaHCO_3$ (10 equiv)	air	100	23
17	$PdCl_2(PPh_3)_2$ (5 mol %)	KF (1 equiv)	air	100	50
18	$PdCl_2(PPh_3)_2$ (100 mol %)	KF (20 equiv)	air	100	95

[a]Conversion based on recovered starting material. [b]Isolated yield.

phosphine ligand suggests that perhaps the ligand structure plays a minimal role in the observed catalytic cycle (*vide infra*).

We next screened the catalyst oxidant based on previously reported boronic acid and ester homocoupling reactions (entries 8−10). Although less mechanistically understood, the oxidative homocoupling of boronic acids and esters under oxygen-free conditions has been explored utilizing a wide variety of chemical oxidants. The most common reagents for simple boronic acid homocouplings are typically benzoquinone[21] and copper(II) salts.[22] Interestingly, these stoichiometric oxidants prove ineffective in this transformation. Although high conversion of starting material was observed, the complex mixture obtained contained no desired product and instead seemed to favor oligomerization as opposed to macrocyclization. This could be related to the first transmetalation step from the proposed palladium peroxide species. As was discussed above, this step is second order in boronic acid or ester. The intramolecular nature of this system could allow for structural preorganization of the boronic esters to facilitate the second order transmetalation step. It is not clear how this mechanistic step would be possible in the absence of oxygen. Additionally, we observed that a rigorously pure oxygen environment does not lead to a significant increase in yield, simplifying the reaction setup (entry 1 vs entry 10).

Initially, we assumed that the role of fluoride in this reaction was to activate the boronic esters to their corresponding fluoroboronates to enhance transmetalation.[12] The Lloyd−Jones group showed in 2010, however, that it was energetically less favorable to transmetallate through such a boronate intermediate and likely boronic acids and esters were directly transmetalated from a palladium hydroxo species.[23] As illustrated in Figure 2, the role of fluoride in this transformation is likely to reduce palladium(II) to palladium(0) through the oxidation of the phosphine ligands to their corresponding phosphine oxides.[19] According to the catalytic cycle proposed by Adamo, there is no inherent need for a fluoride source and the catalytic cycle could begin with the O_2-mediated oxidation of a palladium(0) source. A bis-ligated palladium(0) was shown to undergo oxidation with molecular oxygen to isolable palladium(II) bis(triphenylphosphine)peroxide **3**.[13a] This was theoretically and experimentally shown by Adamo to be the active catalyst in this homocoupling reaction. Additionally, this circumvents the need for fluoride as discussed above and would require only the addition of water as a base in the hydrogen peroxide forming step. We sought to examine whether palladium(0) sources (entries 11−13) in the presence of air could carry out the desired transformation. Table 1 illustrates that in fact palladium(0) can carry out the desired transformation with reasonably similar conversions and yields. Again the conversion and yield do not vary dramatically with the choice of phosphine ligand similar to what was observed in the case of palladium(II) sources. The catalyst described in the work by Adamo, peroxide **3**, was prepared and screened under various conditions (entries 14−16) to determine if in fact this could be a competent catalyst in the desired macrocyclization.[15] Under the standard base-free conditions screened above, moderate conversion and comparable isolated yields of product were observed. However, a lower catalyst loading gave poor conversion indicating poor turnover. The addition of an aqueous base allowed for full conversion but gave poor yields in comparison to the base-free conditions. With these results, we concluded that the palladium peroxide compound could act

DOI: 10.1021/jacs.6b12658
J. Am. Chem. Soc. 2017, 139, 3106−3114

as a competent catalyst as reported by Adamo. Finally, we sought to screen the catalyst loading in entries 17 and 18. Although a full equivalent of palladium (entry 18) gave full conversion and nearly a quantitative yield, the high catalyst dilution and cost on scale render this option impractical. For this reason 5 mol % catalyst (entry 17) was used in all subsequent reactions.

Direct Comparison to Suzuki–Miyaura Cross-Coupling. With these optimized conditions in hand, we initially sought to compare the oxidative homocoupling to a standard Suzuki–Miyaura cross-coupling.[24] Strained macrocycle **4** was first reported by our group in the synthesis of [6]CPP in 2012 (Scheme 1).[25] The limiting step in this synthetic sequence was

Scheme 1. Preparation of Substrates and Direct Comparison of Intramolecular Suzuki–Miyaura Cross-Coupling and Intramolecular Oxidative Homocoupling Methods To Produce Macrocycle 4

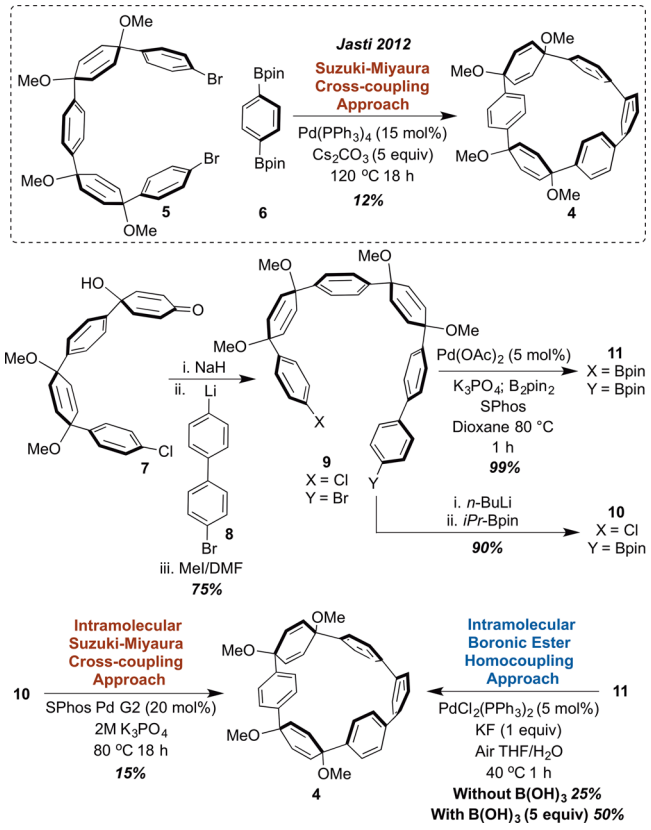

the Suzuki–Miyaura cross-coupling of dibromide **5** and commercially available bisboronate **6**. This method gave macrocycle **4** in a paltry 12% yield. The inherent strain associated with this macrocycle was presumed to be the culprit for this low yield. This macrocycle was chosen as a proving ground for our optimized oxidative homocoupling reaction. In order to make a more direct experimental comparison, the intramolecular Suzuki–Miyaura precursor **10** was synthesized in straightforward fashion. To start, addition of 4′-bromo(1,1′-biphenyl)-4-lithium **8** to previously reported ketone **7**[26] followed by *in situ* methylation of the latent alkoxide delivered bromide **9** in 75% yield. Next, bromide **9** was treated with *n*-butyllithium followed by quenching with 2-isopropoxy-4,4,5,5-tetramethyl-1,3,2-dioxaboralane to deliver boronic ester **10** in 90% yield. Boronic ester homocoupling substrate **11** could also be generated from intermediate **9** by Miyaura borylation[27] in quantitative yield (an alternative route to diboronic ester **11** can be found in the Supporting Information).

The intramolecular Suzuki–Miyaura macrocyclization of Bpin-chloride **10** was rigorously optimized to give macrocycle **4** in 15% yield (Scheme 1), within experimental error for the originally reported Suzuki–Miyaura cross-coupling macrocyclization. The analogous diboronic ester **11** was then subjected to the oxidative homocoupling conditions from entry 17 (Table 1). To our surprise, very little conversion to product was observed after 16 h at room temperature with a mere 5% yield of product **4** isolated. The reaction temperature was then increased to 40 °C. After 1 h, all starting material was consumed and the isolated yield of macrocycle **4** increased to 25%. When the temperature was increased, the major byproduct in these reactions was oxidation of the boronic esters to their corresponding phenols, a common reaction product of boronic acids and esters in the presence of hydrogen peroxide.[28] The catalytic cycle put forth by Adamo generates 1 equiv of hydrogen peroxide per catalyst turnover. We therefore sought to mitigate this decomposition pathway through the sequestration of the generated hydrogen peroxide species using a sacrificial boron source. Although a modest decrease in phenol was observed with various boronic acid pinacol esters such as B_2pin_2 and HBpin, the more reactive boric acid was found to be superior in peroxide sequestration and led to an increase in yield for macrocycle **4** from 5% to 50% (Scheme 1). Of the sacrificial boron sources screened, boric acid is the most cost-effective due to its widespread use as an ant pesticide and is also sufficiently water-soluble to be removed during an aqueous workup. The observed yield of the diboronic ester homocoupling shows a clear advantage in yield, reaction time, and reaction setup over the analogous Suzuki–Miyaura cross-coupling in the synthesis of strained macrocycle **4**.

Direct Comparison to Yamamoto Coupling. With the addition of boric acid to the optimized conditions, we sought to compare the oxidative homocoupling of diboronic esters to the analogous reductive electrophilic aryl bromide homocoupling—the Yamamoto coupling (Scheme 2). Yamago and coworkers impressively demonstrated that an intramolecular aryl

Scheme 2. Direct Comparison of Reductive Yamamoto Coupling of Dibromide 5 and the Oxidative Homocoupling of Diboronic Esters 1 To Form Macrocycle 2

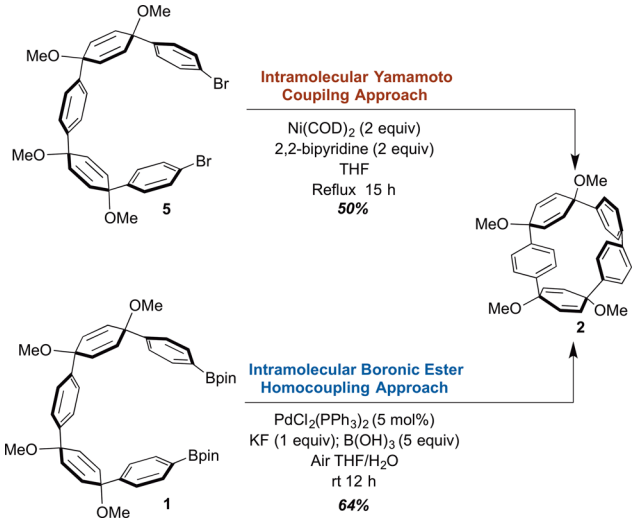

DOI: 10.1021/jacs.6b12658
J. Am. Chem. Soc. 2017, 139, 3106–3114

bromide homocoupling could be used to access macrocycle **2** in 50% yield.[29] The yield in the oxidative homocoupling of substrate **1** to macrocycle **2** increases to 64% under the newly optimized conditions with the addition of boric acid (as compared to original conditions in Figure 1b). Although the yields of the two methods are comparable, its noteworthy that the reaction conditions of the reported Yamamoto reaction require superstoichiometric $Ni(COD)_2$, *in situ* catalyst generation with 2 equiv of 2,2′-bipyridine, and harsh refluxing conditions for 15 h. Moreover, these conditions require a rigorous air- and water-free environment and are most efficiently carried out in a glovebox. In contrast, comparable yields can be obtained with only 5 mol % of palladium at lower reaction times with simple benchtop chemistry without the need to degas solvent or exclude water (see image in Table 1).

Substrate Scope. With standard conditions in hand, we sought to screen several additional substrates to probe the scope of the oxidative homocoupling methodology. In addition to macrocyclic precursors **2** and **4** which lead to [5]- and [6]CPP respectively, we sought to investigate a particularly challenging bent *p*-quaterphenyl precursor **12** toward [7]CPP (Scheme 3). Previous macrocyclic structures with strained *p*-quaterphenyl subunits have been reported by our group with notoriously poor yields that rarely eclipse 15%.[30] The previous synthesis of [7]CPP by our group in 2011 relied on an 8% yielding Suzuki–Miyaura macrocyclization sequence.[31] The Itami group was able to efficiently access a low strained macrocyclic precursor to [7]CPP in 2014 utilizing an intramolecular Yamamoto coupling; however, subsequent low-yielding aromatization produced less than 2 mg of the desired compound.[32] We envisioned a highly strained *p*-quaterphenyl containing [7]CPP macrocyclic precursor **12** which could be accessed using the developed oxidative homocoupling of diboronic ester **15** (Scheme 3). The required diboronic ester precursor **15** was synthesized by the Suzuki–Miyaura cross-coupling of 2 equiv of bromochlorobenzene to diboronic ester **1** in 90% yield. This was then subjected to standard Miyaura borylation conditions to provide diboronic ester **15** in quantitative yield. Seven-ring diboronic ester **15** was then cyclized via oxidative homocoupling to give contorted macrocycle **12** in 35% yield, significantly outperforming previous syntheses.

Scheme 3. Synthesis of Strained *p*-Quaterphenyl Containing Macrocycle 12 via Oxidative Homocoupling of Diboronic Ester 15

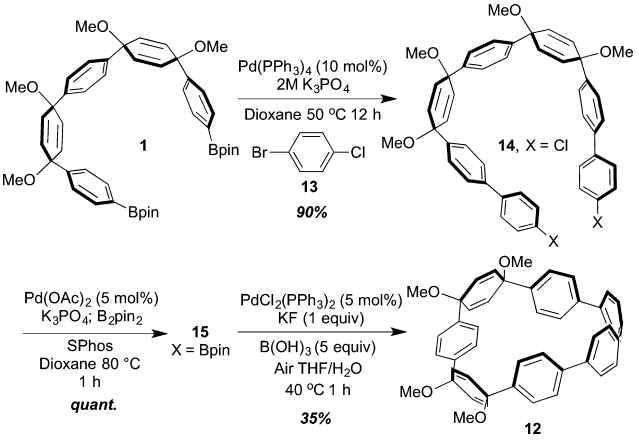

Strained alkynes have been a topic of interest for decades with a recent resurgence due to their applications in bioorthogonal metal-free Huisgen 1,3-dipolar cycloadditions[33] and surface functionalization of materials.[34] We sought to introduce an alkyne into a macrocyclic precursor in order to determine if the oxidative homocoupling methodology could be used to directly access bent alkynes, which often are difficult to prepare in a straightforward manner. The synthetic design of the test substrate was inspired by early work by the Hopf group (Scheme 4).[35] The synthesis of diboronic ester **20** began with lithiation of ethynyltrimethylsilane **16** and nucleophilic addition to silyl protected quinol **17** followed by *in situ* methylation. Potassium carbonate could be added to the reaction to initiate the protodesilation reaction to give deprotected alkyne **18** in quantitative yield. Alkyne **18** was then treated with *n*-butyllithium and added to a second equivalent of protected quinol **17** followed by *in situ* methylation to give alkyne-containing dichloride in 85% yield. This dichloride was then subjected to fluoride-mediated silyl ether deprotection followed by alcohol alkylation to give global methyl ether protected dichloride **19** in 84% yield over three steps. Miyaura borylation of alkyne-containing dichloride **19** gave the desired diboronic ester **20** in quantitative yield. Diboronic ester **20** under optimized room temperature oxidative homocoupling conditions then provided strained alkyne **21** in a remarkable 75% yield. Attempts to isolate the aromatized product **22** were unsuccessful likely due to the highly unstable product even in the presence of trapping agents such as furan. Alkyne **22** is predicted to have over 113 kcal/mol of strain and an internal alkyne angle of 149°, both values exceeding the extremely nonplanar alkyne cyclophanes by Tobe[36] and Kawase.[37] With this methodology in hand, further exploration toward related highly strained alkynes and their application is currently underway.

Scheme 4. Synthesis of Strained Alkyne Containing Macrocycle 21 via Oxidative Homocoupling of Diboronic Ester 20

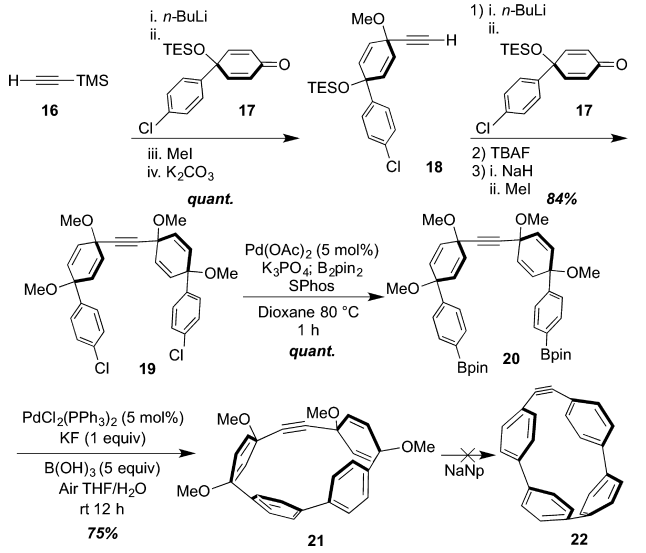

A significant challenge in the synthetic pursuit of cyclophane-containing natural products is often the macrocyclization step.[2a] Biaryl-containing cyclophanes are often ridged, contorted, and conformationally restricted adding considerable challenge in

DOI: 10.1021/jacs.6b12658
J. Am. Chem. Soc. 2017, 139, 3106–3114

the synthetic preparation of these structures. To further prove the versatility of the oxidative homocoupling reaction, we targeted the acerogenin E macrocyclic precursor **23** (Scheme 5). The initial synthesis of this natural product by Usuki[38]

Scheme 5. Formal Synthesis of Acerogenin E Utilizing an Oxidative Homocoupling of Diboronic Ester 27

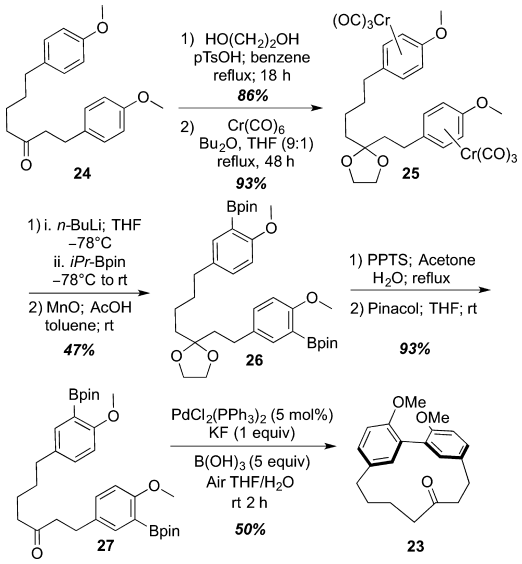

relied on an intramolecular Suzuki−Miyaura coupling to construct the cyclic architecture of this molecule. This late stage coupling proved to be the limiting step of the formal synthesis giving the desired macrocycle in 34% yield after rigorous optimization. These optimized conditions were run under an inert atmosphere at refluxing conditions for 24 h. Our synthesis began with the previously reported intermediate **24**. After glycol protection of the ketone, treatment of this compound with $Cr(CO)_6$ gave metalated **25** in 93% yield. This intermediate was then borylated by deprotonation at the ortho-positions with *n*-butyllithium at −78 °C followed by quenching with isopropoxy-4,4,5,5-tetramethyl-1,3,2-dioxaborolane to give **28** in 47% yield following demetalation. Deprotection of the ketone using standard conditions then provided diboronic ester **27** after reprotection of the resulting boronic acids with pinacol. Gratifyingly, after subjecting diboronic ester **27** to our optimized oxidative homocoupling conditions at room temperature for 2 h, the desired macrocycle **23** was isolated in 50% yield. Further analysis of the product is provided in subsequent sections.

Single crystals of macrocycles **2**, **12**, **21**, and **23** were obtained in order to assess the structural deformation in each compound. Note that crystal structure **4** was previously published and is available through the Cambridge Crystallographic Data Centre (CCDC No. 852988).[25] ORTEP models of each structure are shown in Table 2. In order to account for disorder or the additional impact of packing forces, each molecule was also computationally minimized (B3LYP/6-31d*) and resulted in comparable geometric values (Supporting Information, Supporting Tables 2−6). Additionally, homodesmotic reactions for each macrocycle were carried out computationally to provide a relative estimate of macrocycle strain energy.[31,39] Based on homodesmotic reactions, we observe a gradual increase in strain with macrocycles **2**, **4**, **12**, and **21** with strain energies of 28, 38, 41, and 45 kcal/mol, respectively. Interestingly, macrocycle **23** is relatively strain-free (4 kcal/mol) but exhibits atropisomerism via ^{1}H NMR studies (Supporting Information, Supporting Figure 2). Analysis of the strain per backbone carbon provides an additional metric for estimating the strain building capability of this reaction. These

Table 2. Solid State Analysis of Macrocycles 2, 4, 12, 21, and 23[a]

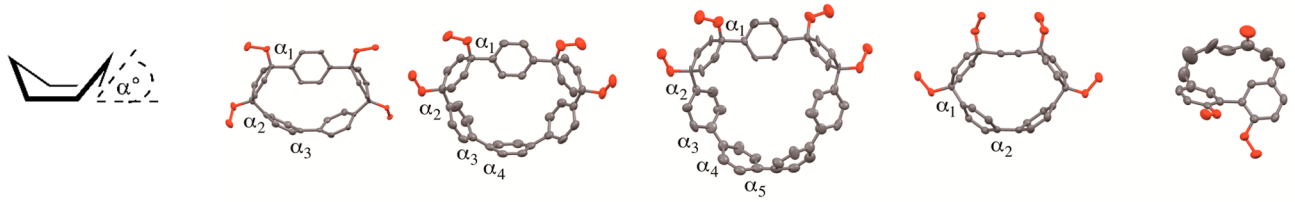

	2	4	12	21	23
Calculated Total Strain (kcal/mol)	28	38	41	45	4.0
Backbone Carbon[b]	30	36	42	26	19
Strain per Backbone Carbon ((kcal/mol)/C)	0.93	1.1	0.98	1.7	0.21
α_1	2.1	2.6	3.5	12	NA
α_2	12	8.0	4.1	14	NA
α_3	12	8.9	4.9	NA	NA
α_4	NA	13	13	NA	NA
α_5	NA	NA	13	NA	NA
Alkyne Angle	NA	NA	NA	6.3	NA

[a]α represents the distortion of an aryl ring out of planarity. All strain calculations are B3LYP/6-31g(d). [b]Backbone carbons are shown in gray.

DOI: 10.1021/jacs.6b12658
J. Am. Chem. Soc. 2017, 139, 3106−3114

values range from 0.93 kcal/mol per backbone carbon up to 1.7 kcal/mol per backbone carbon for **21**. For perspective, [12]CPP, which is synthesized using a high temperature Suzuki–Miyaura cross-coupling and a highly exothermic reductive aromatization protocol, registers at 0.67 (kcal/mol) per backbone carbon. The oxidative homocoupling reaction can generate these types of strained compounds directly at low temperatures. Impressively, the strain of alkyne macrocycle **21** falls between average strain per backbone carbon in [8]CPP (1.5 (kcal/mol)/carbon) and [7]CPP (2.0 (kcal/mol)/carbon).[7b] Furthermore, the benzene displacement angle α is a measure of how bent a benzene ring is from planarity and another metric for molecular strain. As a frame of reference, the bent benzene in haouamine A has an α of 14°.[40] There is a large variation in α for macrocycles **2**, **4**, **12**, and **21** with peak values between 13° and 14°. In addition to the α displacement, the alkyne in macrocycle **21** is distorted by 6° toward the center of the macrocycle.

Mechanistic Studies. In order to gain further insight into the operating mechanism, we first turned to NMR experiments. Adamo showed that, in the case of boronic acids, the catalytic cycle could be manipulated to observe various intermediates.[13a] First, when an excess of boronic acid was used relative to the palladium peroxide **3**, boronate coordination is observed. The coordination event can be pushed to the first transmetalation event by the addition of excess boronic acid relative to the palladium. This unique transmetalation is second order in the boronic acid and was supported by kinetic data. Next an accumulation of the palladium hydroxide intermediate is observed (step **D**, Figure 2). This is followed by a transmetalation and reductive elimination akin to that of the Suzuki–Miyraura cross-coupling. In our case, the two boronic esters are tethered and are conformationally flexible enough to interact with a single palladium center. This conformational proximity might act to "preorganize" each boronic ester to favor the first transmetalation, which had been shown to be second order in the intermolecular case.

To explore these mechanistic steps, we carried out a set of NMR experiments in air-saturated d_8 THF. First, we qualitatively tracked the conversion of diboronic ester **1** to macrocycle **2** using the optimized conditions at room temperature (Figure 3). Diboronic ester **1** and $PdCl_2(PPh_3)_2$ were dissolved in d_8 THF to produce an initial NMR spectrum (t_0) before fluoride activation. Potassium fluoride in D_2O was then injected followed by a collection of the spectrum. At this initial time point (t_1), we observed no product formation; however, new signals consistent with the formation of triphenylphosphine oxide were apparent with presumably concomitant formation of Pd(0) from $PdCl_2(PPh_3)_2$. Within 20 min, we began to observe product formation. Time points are taken every 20 min for 2 h and finally an end point is taken at 12 h, showing full conversion of starting material. At no point during this reaction do we observe any signals indicative of the formation of a palladium hydroxide intermediate nor do we observe signals associated with a bis(aryl) Pd(II) prereductive elimination step. The induction period observed upon addition of fluoride followed by rapid substrate conversion was initially attributed to the reduction of Pd(II) to Pd(0) and phosphine oxidation formation.

In order to gain further insight, we decided to qualitatively assess the reduction of $PdCl_2(PPh_3)_2$ with *in situ* fluoride activation by ^{1}H NMR. Tetrabutylammonium fluoride was chosen to avoid any miscibility issues. Figure 4 shows unbound

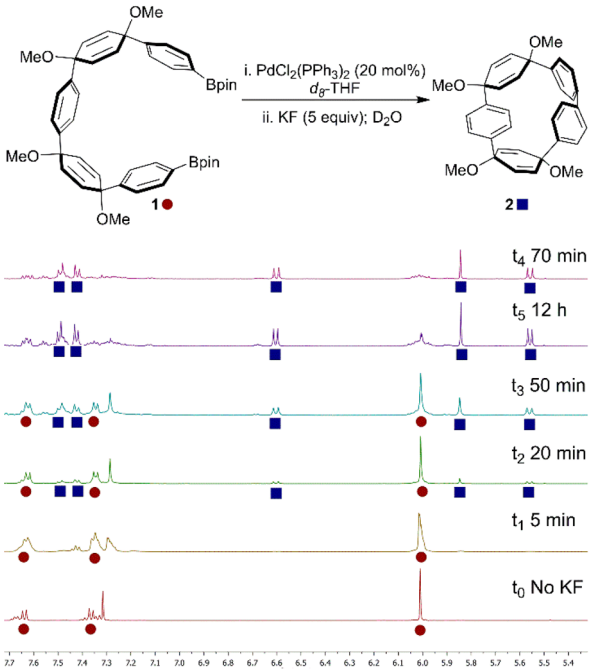

Figure 3. Profile of reaction mixture by ^{1}H NMR over multiple time points.

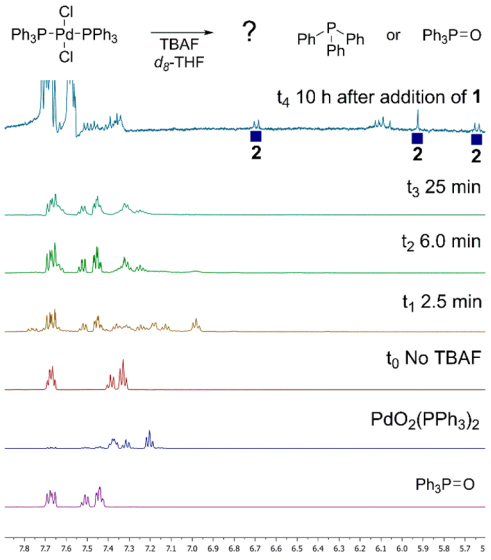

Figure 4. *In situ* reduction of $PdCl_2(PPh_3)_2$ using TBAF in d_8 THF.

triphenylphosphine, triphenylphosphine oxide, and peroxo palladium species **3** for reference. At t_0, no fluoride is present; the spectrum only contains peaks associated with $PdCl_2(PPh_3)_2$. The spectrum shows 2 min after fluoride addition (t_1) the disappearance of the parent complex entirely and a complicated spectrum with several species emerging. The most prominent species observed are consistent with triphenylphosphine oxide. By 6 min (t_2) we observe near-quantitative conversion to triphenylphosphine oxide with no apparent formation of peroxo species **3**. This spectrum remains relatively unchanged over the remaining time points t_3 and t_4. At 90 min solid substrate **1** was added to the NMR tube along with water. After 12 h the crude NMR (Figure 4) shows complete consumption of diboronic ester **1** and conversion to macrocycle **2**. These results and those shown in Figure 3 have

DOI: 10.1021/jacs.6b12658
J. Am. Chem. Soc. 2017, 139, 3106–3114

led us to speculate that perhaps the discrete peroxo palladium complex **3** is not being generated, but rather initially full oxidation of phosphine ligands leaves a bare ligandless palladium species. Under these oxidative conditions palladium nanoparticles are known to form.[41] Heterogeneous catalysis also typically shows induction periods followed by rapid conversion to product, similar to what was observed in our studies (Figure 3). Intriguingly, gold nanoparticles have been shown to effectively carry out the oxidative homocoupling of boronic esters.[42]

Dynamic light scattering (DLS) was used to further probe the possibility of nanoparticle generation. Similar conditions to the NMR experiments above were used to generate the nanoparticles *in situ* (Figure 5a). Particles on the order of 0.5−5

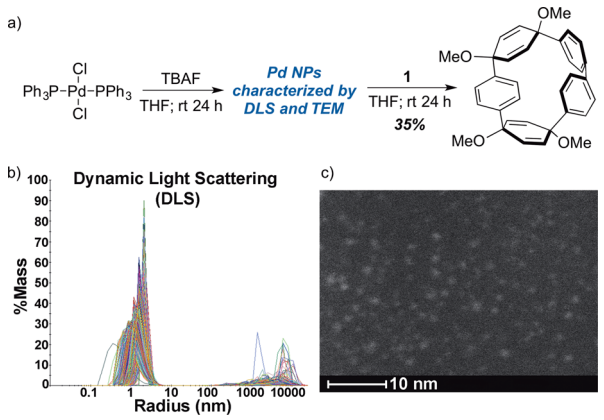

Figure 5. (a) *In situ* reduction of $PdCl_2(PPh_3)_2$ using TBAF in THF, (b) DLS of resulting species, projected stack of 30 s acquisitions over 24 h,[41] and (c) dark field TEM images of resulting palladium species.

nm in diameter are immediately present upon addition of TBAF to a solution of catalyst (Supporting Information, Supporting Figures 14−18). This size regime persists over 24 h (Figure 5b) and gradually shows a shift to larger particles (50−100 nm) over 48 h. The solution produced after 24 h was also analyzed by transmission electron microscopy (TEM). The dark field (Figure 5c) shows evenly dispersed particles between 1 and 5 nm in diameter, consistent with DLS measurements. The same stock solution used to image the nanoparticles was then diluted to 1 mM with the addition of approximately 10% THF/H_2O by volume to simulate the reaction conditions used in the oxidative homocoupling. Diboronic ester **1** was then added without any additional base or boric acid and gave full conversion of substrate and an isolable 30% yield of product after 24 h. This supports the possibility that nanoparticles serve as the active catalytic species in reaction, but does not rule out equilibrium monomeric species. More detailed studies are underway to explore this possibility.

CONCLUSION

In conclusion we have reported an exceptionally mild oxidative homocoupling of aryl boronic esters to form strained and conformationally restricted macrocycles. The hallmarks of this process are the simple reaction setup, short reaction times, and low temperatures. This methodology serves to compliment the more widely employed nucleophile−electrophile cross-coupling and electrophile-electrophile homocoupling, but with some noteworthy advantages. The oxidative homocoupling was shown to outperform Suzuki−Miyaura cross-coupling and is more economically viable and simpler operationally than the Yamamoto coupling to prepare comparable structures. Additionally, the recent increase in methodologies allowing direct access to boronic acids and esters without the need for halogenated intermediates provides greater impetus to further explore this transformation. Although the reaction may follow the proposed mechanism put forth by Adamo in 2005, ^1H NMR and DLS data suggest the possibility that this reaction may proceed via a heterogeneous palladium nanoparticle pathway. Further studies are underway to understand the mechanistic possibility of this supposition. With the ability to build more strained and conformationally restricted molecules at significantly lower temperature, we anticipate this reaction will find application across many disciplines including medicinal, materials, and supramolecular chemistry.

ASSOCIATED CONTENT

Supporting Information

The Supporting Information is available free of charge on the ACS Publications website at DOI: 10.1021/jacs.6b12658.

Crystallographic data for **2** (CIF)
Crystallographic data for **12** (CIF)
Crystallographic data for **19** (CIF)
Crystallographic data for **21** (CIF)
Crystallographic data for **23** (CIF)
General synthetic details, NMR spectra, VT NMR spectra, crystallographic details, computational details, and DLS figures (PDF)

AUTHOR INFORMATION

Corresponding Author

*rjasti@uoregon.edu

ORCID

Evan R. Darzi: 0000-0002-6900-2229
Ramesh Jasti: 0000-0002-8606-6339

Notes

The authors declare no competing financial interest.

ACKNOWLEDGMENTS

Financial support was provided by the National Science Foundation (CHE-1255219), the Sloan Foundation, the Camille and Henry Dreyfus Foundation, and generous startup funds from the University of Oregon. The NMR facilities at the University of Oregon are supported by the NSF (CHE-1427987). HRMS data were obtained at the Mass Spectrometry Facility in the Department of Chemistry at the University of California, Irvine by Dr. Jon Greaves. Dr. Paul Evans is acknowledged for the synthesis of **32**. Brantly Fulton is acknowledged for experimental assistance with DLS data acquisition. The Center for Advanced Materials Characterization in Oregon (CAMCOR) and Joshua Razink are acknowledged for the acquisition of TEM images.

REFERENCES

(1) (a) Nguyen, S. T.; Johnson, L. K.; Grubbs, R. H.; Ziller, J. W. *J. Am. Chem. Soc.* **1992**, *114* (10), 3974−3975. (b) Bielawski, C. W.; Grubbs, R. H. *Prog. Polym. Sci.* **2007**, *32* (1), 1−29. (c) Schrock, R. R. *Acc. Chem. Res.* **1990**, *23* (5), 158−165. (d) Schrock, R. R.; Hoveyda, A. H. *Angew. Chem., Int. Ed.* **2003**, *42* (38), 4592−4633.
(2) (a) Gulder, T.; Baran, P. S. *Nat. Prod. Rep.* **2012**, *29* (8), 899−934. (b) Villar, E. A.; Beglov, D.; Chennamadhavuni, S.; Porco, J. A.,

DOI: 10.1021/jacs.6b12658
J. Am. Chem. Soc. 2017, 139, 3106−3114

Jr; Kozakov, D.; Vajda, S.; Whitty, A. *Nat. Chem. Biol.* **2014**, *10* (9), 723−731.
(3) (a) Xia, J.; Bacon, J. W.; Jasti, R. *Chem. Sci.* **2012**, *3* (10), 3018−3021. (b) Iwamoto, T.; Watanabe, Y.; Takaya, H.; Haino, T.; Yasuda, N.; Yamago, S. *Chem. - Eur. J.* **2013**, *19* (42), 14061−14068. (c) Iwamoto, T.; Watanabe, Y.; Sadahiro, T.; Haino, T.; Yamago, S. *Angew. Chem., Int. Ed.* **2011**, *50* (36), 8342−8344. (d) Iwamoto, T.; Slanina, Z.; Mizorogi, N.; Guo, J.; Akasaka, T.; Nagase, S.; Takaya, H.; Yasuda, N.; Kato, T.; Yamago, S. *Chem. - Eur. J.* **2014**, *20* (44), 14403−14409. (e) Matsuno, T.; Sato, S.; Iizuka, R.; Isobe, H. *Chem. Sci.* **2015**, *6* (2), 909−916. (f) Sato, S.; Yamasaki, T.; Isobe, H. *Proc. Natl. Acad. Sci. U. S. A.* **2014**, *111* (23), 8374−8379. (g) Isobe, H.; Hitosugi, S.; Yamasaki, T.; Iizuka, R. *Chem. Sci.* **2013**, *4* (3), 1293−1297. (h) Hitosugi, S.; Iizuka, R.; Yamasaki, T.; Zhang, R.; Murata, Y.; Isobe, H. *Org. Lett.* **2013**, *15* (13), 3199−3201.
(4) (a) Burns, N. Z.; Krylova, I. N.; Hannoush, R. N.; Baran, P. S. *J. Am. Chem. Soc.* **2009**, *131* (26), 9172−9173. (b) Baran, P. S.; Burns, N. Z. *J. Am. Chem. Soc.* **2006**, *128* (12), 3908−3909.
(5) (a) Lloyd-Williams, P.; Giralt, E. *Chem. Soc. Rev.* **2001**, *30* (3), 145−157. (b) Evans, D. A.; Wood, M. R.; Trotter, B. W.; Richardson, T. I.; Barrow, J. C.; Katz, J. L. *Angew. Chem., Int. Ed.* **1998**, *37* (19), 2700−2704. (c) Nicolaou, K. C.; Li, H.; Boddy, C. N. C.; Ramanjulu, J. M.; Yue, T.-Y.; Natarajan, S.; Chu, X.-J.; Bräse, S.; Rübsam, F. *Chem. - Eur. J.* **1999**, *5* (9), 2584−2601. (d) Boger, D. L.; Miyazaki, S.; Kim, S. H.; Wu, J. H.; Castle, S. L.; Loiseleur, O.; Jin, Q. *J. Am. Chem. Soc.* **1999**, *121* (43), 10004−10011.
(6) Cram, D. J.; Cram, J. M. *Acc. Chem. Res.* **1971**, *4* (6), 204−213.
(7) (a) Golder, M. R.; Jasti, R. *Acc. Chem. Res.* **2015**, *48* (3), 557−566. (b) Darzi, E. R.; Jasti, R. *Chem. Soc. Rev.* **2015**, *44* (18), 6401−6410.
(8) Negishi, E.-i. *Handbook of Organopalladium Chemistry for Organic Synthesis*; John Wiley & Sons: New York, 2002; Vol. *1*.
(9) Evans, P. J.; Darzi, E. R.; Jasti, R. *Nat. Chem.* **2014**, *6* (5), 404−408.
(10) Dhital, R. N.; Sakurai, H. *Asian J. Org. Chem.* **2014**, *3* (6), 668−684.
(11) (a) Iafe, R. G.; Kuo, J. L.; Hochstatter, D. G.; Saga, T.; Turner, J. W.; Merlic, C. A. *Org. Lett.* **2013**, *15* (3), 582−585. (b) Iafe, R. G.; Chan, D. G.; Kuo, J. L.; Boon, B. A.; Faizi, D. J.; Saga, T.; Turner, J. W.; Merlic, C. A. *Org. Lett.* **2012**, *14* (16), 4282−4285.
(12) Moreno-Mañas, M.; Pérez, M.; Pleixats, R. *J. Org. Chem.* **1996**, *61* (7), 2346−2351.
(13) (a) Adamo, C.; Amatore, C.; Ciofini, I.; Jutand, A.; Lakmini, H. *J. Am. Chem. Soc.* **2006**, *128* (21), 6829−6836. (b) Lakmini, H.; Ciofini, I.; Jutand, A.; Amatore, C.; Adamo, C. *J. Phys. Chem. A* **2008**, *112* (50), 12896−12903.
(14) Yoshida, H.; Yamaryo, Y.; Ohshita, J.; Kunai, A. *Tetrahedron Lett.* **2003**, *44* (8), 1541−1544.
(15) Liu, Q.; Li, G.; He, J.; Liu, J.; Li, P.; Lei, A. *Angew. Chem., Int. Ed.* **2010**, *49* (19), 3371−3374.
(16) (a) Carrow, B. P.; Hartwig, J. F. *J. Am. Chem. Soc.* **2011**, *133* (7), 2116−2119. (b) Lennox, A. J. J.; Lloyd-Jones, G. C. *Angew. Chem., Int. Ed.* **2013**, *52* (29), 7362−7370.
(17) Braga, A. A. C.; Ujaque, G.; Maseras, F. *Organometallics* **2006**, *25* (15), 3647−3658.
(18) Thomas, A. A.; Denmark, S. E. *Science* **2016**, *352* (6283), 329−332.
(19) (a) Mason, M. R.; Verkade, J. G. *Organometallics* **1992**, *11* (6), 2212−2220. (b) McLaughlin, P. A.; Verkade, J. G. *Organometallics* **1998**, *17* (26), 5937−5940.
(20) Lanci, M. P.; Brinkley, D. W.; Stone, K. L.; Smirnov, V. V.; Roth, J. P. *Angew. Chem., Int. Ed.* **2005**, *44* (44), 7273−7276.
(21) Yamamoto, Y. *Synlett* **2007**, *2007* (12), 1913−1916.
(22) Miyaura, N.; Suzuki, A. *Main Group Met. Chem.* **1987**, *10* (5), 295−300.
(23) (a) Butters, M.; Harvey, J. N.; Jover, J.; Lennox, A. J. J.; Lloyd-Jones, G. C.; Murray, P. M. *Angew. Chem., Int. Ed.* **2010**, *49* (30), 5156−5160. (b) Lennox, A. J. J.; Lloyd-Jones, G. C. *Chem. Soc. Rev.* **2014**, *43* (1), 412−443.
(24) Miyaura, N.; Yanagi, T.; Suzuki, A. *Synth. Commun.* **1981**, *11* (7), 513−519.
(25) Xia, J.; Jasti, R. *Angew. Chem., Int. Ed.* **2012**, *51* (10), 2474−2476.
(26) Li, P.; Sisto, T. J.; Darzi, E. R.; Jasti, R. *Org. Lett.* **2014**, *16* (1), 182−185.
(27) (a) Takagi, J.; Takahashi, K.; Ishiyama, T.; Miyaura, N. *J. Am. Chem. Soc.* **2002**, *124* (27), 8001−8006. (b) Billingsley, K. L.; Barder, T. E.; Buchwald, S. L. *Angew. Chem., Int. Ed.* **2007**, *46* (28), 5359−5363.
(28) Ainley, A. D.; Challenger, F. *J. Chem. Soc.* **1930**, 2171−2180.
(29) (a) Kayahara, E.; Patel, V. K.; Yamago, S. *J. Am. Chem. Soc.* **2014**, *136* (6), 2284−2287. (b) Patel, V. K.; Kayahara, E.; Yamago, S. *Chem. - Eur. J.* **2015**, *21* (15), 5742−5749.
(30) Darzi, E. R.; Sisto, T. J.; Jasti, R. *J. Org. Chem.* **2012**, *77* (15), 6624−6628.
(31) Sisto, T. J.; Golder, M. R.; Hirst, E. S.; Jasti, R. *J. Am. Chem. Soc.* **2011**, *133* (40), 15800−15802.
(32) Sibbel, F.; Matsui, K.; Segawa, Y.; Studer, A.; Itami, K. *Chem. Commun.* **2014**, *50* (8), 954−956.
(33) (a) Agard, N. J.; Prescher, J. A.; Bertozzi, C. R. *J. Am. Chem. Soc.* **2004**, *126* (46), 15046−15047. (b) Laughlin, S. T.; Baskin, J. M.; Amacher, S. L.; Bertozzi, C. R. *Science* **2008**, *320* (5876), 664−667.
(34) Iha, R. K.; Wooley, K. L.; Nyström, A. M.; Burke, D. J.; Kade, M. J.; Hawker, C. J. *Chem. Rev.* **2009**, *109* (11), 5620−5686.
(35) Srinivasan, M.; Sankararaman, S.; Hopf, H.; Varghese, B. *Eur. J. Org. Chem.* **2003**, *2003* (4), 660−665.
(36) Nobusue, S.; Yamane, H.; Miyoshi, H.; Tobe, Y. *Org. Lett.* **2014**, *16* (7), 1940−1943.
(37) Kawase, T.; Darabi, H. R.; Oda, M. *Angew. Chem., Int. Ed. Engl.* **1996**, *35* (22), 2664−2666.
(38) Ogura, T.; Usuki, T. *Tetrahedron* **2013**, *69* (13), 2807−2815.
(39) Jasti, R.; Bhattacharjee, J.; Neaton, J. B.; Bertozzi, C. R. *J. Am. Chem. Soc.* **2008**, *130* (52), 17646−17647.
(40) Garrido, L.; Zubía, E.; Ortega, M. J.; Salvá, J. *J. Org. Chem.* **2003**, *68* (2), 293−299.
(41) (a) Han, W.; Liu, C.; Jin, Z.-L. *Org. Lett.* **2007**, *9* (20), 4005−4007. (b) Zalesskiy, S. S.; Ananikov, V. P. *Organometallics* **2012**, *31* (6), 2302−2309.
(42) (a) Tsunoyama, H.; Sakurai, H.; Ichikuni, N.; Negishi, Y.; Tsukuda, T. *Langmuir* **2004**, *20* (26), 11293−11296. (b) Sophiphun, O.; Wittayakun, J.; Dhital, R. N.; Haesuwannakij, S.; Murugadoss, A.; Sakurai, H. *Aust. J. Chem.* **2012**, *65* (9), 1238−1243. (c) Karanjit, S.; Ehara, M.; Sakurai, H. *Chem. - Asian J.* **2015**, *10* (11), 2397−2403.

DOI: 10.1021/jacs.6b12658
J. Am. Chem. Soc. 2017, 139, 3106−3114